As now we have the data from the November 2018 experimental run, I set out to trawl through the data files and find some that can be compared to the output my calculations produce. The theory I now use is a 2D (azimuthally symmetric, $z$ and $r$ coordinates) pseudospectral code - I put a fairly detailed description/derivation on arXiv.org [1]. I assume a Gaussian beam (TEM00 mode) and a $\text{sech}(t/\tau)$ type temporal dependence of the field amplitude initially. I will first discuss the initial parameters that my calculations need and how I obtained these from the experimental data files, then provide tables with the precise parameters. In these tables I will also indicate precisely which file I used by name, without the initial "dataset" left off for brevity. Since each single experimental data file contains the data of 10 consecutive measurements, I will have to use mean values for my simulations, but I will indicate the uncertainty of these parameters where it is over 1%. (I don't have the resources to run calculations for each single experimental parameter set - but I don't think that this is necessary either.)

## Input parameters

The input parameters that I need for my simulations are the rubidium vapor density $\mathcal{N}$, the pulse energy $E_0$, the pulse duration $T_{pulse}$ (related to the $\tau$ in the sech function as $T_{pulse} = \tau \cdot 2 \cdot \text{acosh}(\sqrt{2})$ ), the beam diameter $d_0$ of the Gaussian beam at the beam waist (FWHM of intensity - this is related to the beam waist parameter $w_0$ as $d_0 = w_0 \sqrt{2 \cdot \log(2)}$) ) and finally the location of the beam waist $z_0$ (in the absence of rubidium of course). Here are some comments on each of these parameters.

- The easiest case by far is the vapor density $\mathcal{N}$. They can be found in the *rbDens_value* variable of the data files, they are very stable (constant accross the measurements) and almost the same at the two locations along the cell. I will just use the mean value of the two locations, averaged over the measurements.

- The initial pulse energy is also not problematic if we believe the calibration of the data found in the *Emeter04* variables, which is the input energy. It can be considerably less than the "nickname" of the data files (e.g. "_120mJ"), but it is stable and we'll trust Emeter04 as Josh suggested.

- Somewhat more problematic is the pulse duration $T_{pulse}$. The autocorrelator is placed after the cell, so it measures the output pulse length. We can get an idea of the ingoing pulse length from the vacuum measurements, but these are only available for four pulse energies, 20 mJ, 40 mJ, 80 mJ and 120 mJ. The variable *autoCorrWid* contains the $\tau$ of a sech function fit to the autocorrelation signal and $T_{pulse}$ can extracted from that. Because there is a systematic change with pulse energy larger than the measurement fluctuations (less energy results in a "shorter" pulse), I used the four values measured in vacuum for the 20, 40, 80 and 120 mJ pulses and used the mean of the neighbouring values for the 60 and 100 mJ pulses. Also I used the 20 mJ value for the 5-10 mJ pulses. I realized later that this process is not very accurate because pulses tagged "100 mJ"

---

[1] arXiv:1902.09281

sometimes have less than 90 mJ energy in reality so a proper calibration curve should have been constructed and a proper linear interpolation between the known values used. However I wanted to stay consistent and not change methodology on the run so the pulse durations are now the same for the pulses named "100 mJ" regardless of the real measured energy. Overall, pulse duration is a parameter that is not very accurate anyway, they fluctuate from measurement to measurement even in the same set. The measured values are set with red in the table and their uncertainty indicated.

- Beam width and waist location parameters were obtained the following way: I took the three virtual camera pictures Vcam3, Vcam4 and Vcam5 which are supposed to give us the energy distribution of the beam at the entrance, center and exit of the cell in vacuum, removed the hot pixels and fitted each with a simple azimuthally symmetric Gaussian distribution

$$I(x, y) = I_0 \exp\left(-2[(x - x_0)^2 + (y - y_0)^2]/w(z)^2\right).$$

Having obtained the three values $w(0)$, $w(5)$ and $w(10)$, I used them in a nonlinear fit again using the Gaussian beam formula

$$w(z) = w_0\sqrt{(1 + (z - z_0)^2/z_R^2)}$$

to obtain the $w_0$ and $z_0$ parameters of the beam. (The other parameters, $I_0$, $x_0$ and $y_0$ are not used.) Again, I perfomed the fit for each of the 10 pulses in a series and then averaged over the values. $w_0$ (and hence $d_0$) is fairly consistent but $z_0$ fluctuates quite a bit because we are trying to tell the waist location from three values close to it.

Finally, here is the table for the parameters of the first set of calculations. The parameters have been rounded in the table (well within the limits of the displayed experimental uncertainty).

Input parameters for the set of calculations with $\mathcal{N} = 2 \cdot 10^{14}$

| name | $\mathcal{N}[10^{14}/cm^3]$ | $E_0$ [mJ] | $T_{pulse}$ [fs] | $d_0$ [mm] | $z_0$ [m] | exp. data |
|------|------|------|------|------|------|------|
| 5_01 | 1.887 | 4.84 ± 0.12 | 99.4 | 1.851 ± 0.024 | 8.35 ± 1.34 | Rb2e14_5mJ |
| 6_01 | 1.890 | 6.47 ± 0.20 | 99.4 | 1.850 ± 0.022 | 9.33 ± 1.52 | Rb2e14_6mJ |
| 10_01 | 1.886 | 10.22 ± 0.17 | 99.4 | 1.855 ± 0.029 | 8.57 ± 1.41 | Rb2e14_10mJ |
| 20_01 | 1.889 | 20.08 ± 0.37 | 99.4 ± 5.5 | 1.865 ± 0.047 | 8.31 ± 1.40 | Rb2e14_20mJ |
| 40_01 | 1.891 | 38.9 ± 0.66 | 115.21 ± 7.2 | 1.846 ± 0.025 | 8.46 ± 1.09 | Rb2e14_40mJ |
| 60_01 | 1.889 | 57.63 ± 0.97 | 119.45 | 1.844 ± 0.027 | 7.96 ± 1.21 | Rb2e14_60mJ |
| 80_01 | 1.887 | 77.07 ± 2.15 | 123.7 ± 4.3 | 1.880 ± 0.031 | 8.22 ± 1.30 | Rb2e14_80mJ |
| 100_01 | 1.888 | 95.83 ± 1.78 | 125.59 | 1.827 ± 0.027 | 7.48 ± 0.85 | Rb2e14_100mJ |
| 120_01 | 1.887 | 112.15 ± 1.89 | 127.47 ± 10.3 | 1.803 ± 0.04 | 6.71 ± 0.94 | Rb2e14_120mJ |

# Computer output vs. experimental data

## Outgoing pulse energy

Now comes the interesting part, comparing what was measured to what I calculated. First and simplest, the measured energy of the transmitted pulse is

considered. The comparison is complicated by the observation that the output of the downstream energy meter (*Emeter03* variable in the data files) is sometimes considerably higher for vacuum measurements than that of the input energy meter to which we adjusted the input pulse energy of the computation. The table below shows this:

*Input and output energy for vacuum measurements.*

| name | Emeter04 | Emeter03 | Emeter04/Emeter03 |
|------|----------|----------|-------------------|
| "Vac_20mJ" | $20.54 \pm 0.43$ | $27.46 \pm 0.62$ | $0.748 \pm 0.0046$ |
| "Vac_40mJ" | $40.93 \pm 0.69$ | $47.45 \pm 1.64$ | $0.863 \pm 0.019$ |
| "Vac_80mJ" | $79.96 \pm 0.91$ | $81.69 \pm 2.77$ | $0.980 \pm 0.028$ |
| "Vac_120mJ" | $118.01 \pm 1.89$ | $115.12 \pm 2.83$ | $1.025 \pm 0.018$ |

Evidently there is systematic discrepancy much larger than the 1-3% measurement to measurement error for the 20 and 40 mJ pulses propagating in vacuum, but the cause is not clear. For now, I choose to use the data in this table to construct a 'calibration curve'. I use the factors in the last column (and interpolated values) to multiply the measured output energy so that 'vacuum' measurements are scaled to $E_{in} = E_{out}$. The calibration curve is extrapolated to 5-6 mJ energies as well and is shown below:
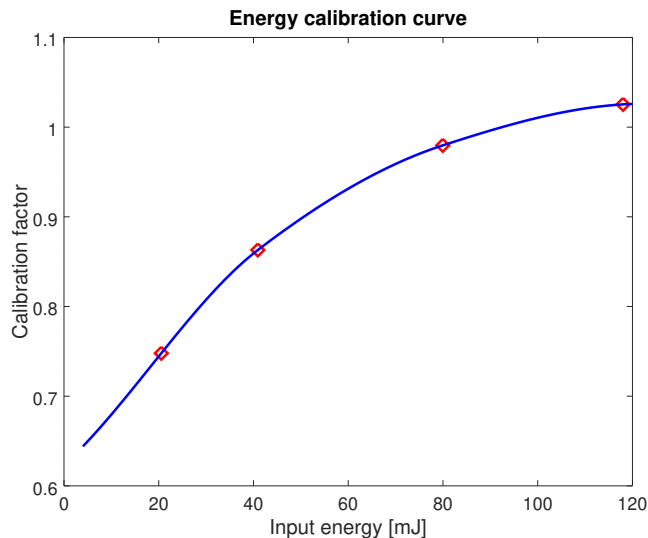


Figure 1: Energy calibration curve for output energy meter. Red diamonds mark the calibration points obtained from the vacuum measurements.
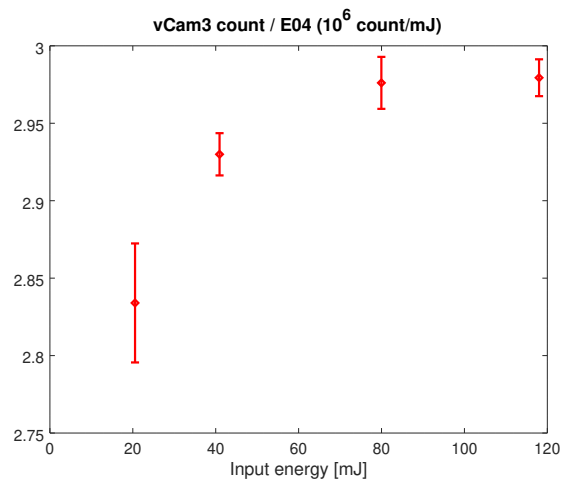
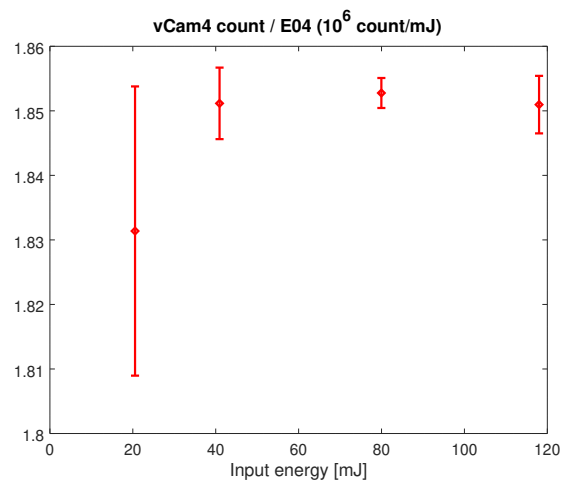Figure 2: Camera count per input energy.



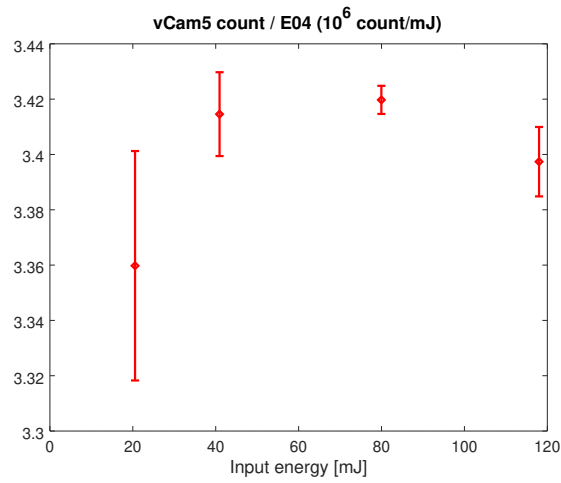Figure 3: Camera count per input energy.
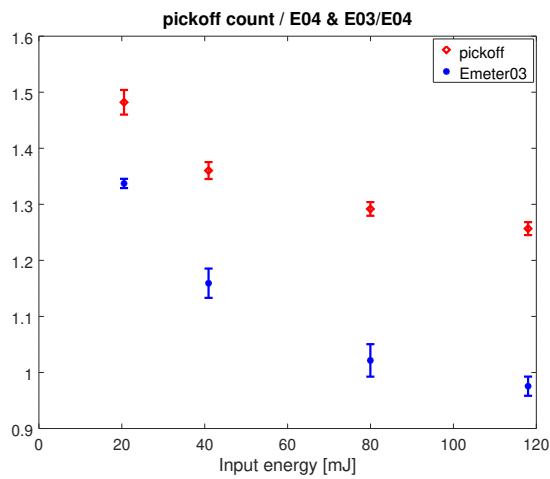
Figure 4: Camera count per input energy.



Figure 5: Camera count per input energy.

Finally, here is the output energy vs. input energy of the pulses for the *Rb2e14* set of simulations, the left panel is the entire set, the right panel is a magnification of the lowest part of the plot. The errors of the experimental data were calculated only from the measurement data set, they do not include the error of the calibration factor.
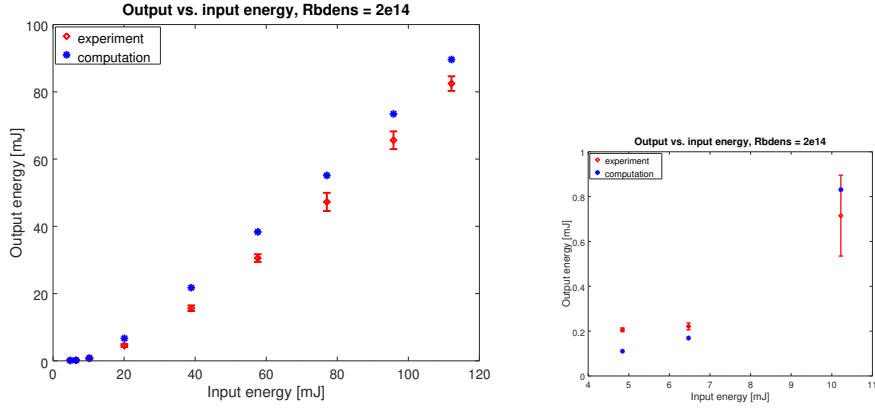
*Output energy of simulation and experiment*

Figure 6: Outgoing pulse energy vs. input pulse energy, left panel is the complete plot, right panel is the lowest three points magnified.

| $E_0$ | $E_{out}$ exp. [mJ] | $E_{out}$ simulation [mJ] |
|-------|--------------------|--------------------------|
| 4.84   | 0.206 | 0.110 |
| 6.47   | 0.221 | 0.169 |
| 10.22  | 0.72  | 0.83  |
| 20.08  | 4.56  | 6.68  |
| 38.89  | 15.64 | 21.75 |
| 57.63  | 30.56 | 38.34 |
| 77.07  | 47.26 | 55.14 |
| 95.83  | 65.59 | 73.43 |
| 112.15 | 82.45 | 89.60 |

## Outgoing beam width

This another parameter that we can try to match between experiment and calculation. To do this, we first have to calibrate the picture of the pickoff camera. As I understand, cameras in the virtual line have no optics in front of them, the size of the laser beam energy distribution can simply be calculated by multiplying the pixel numbers by the 5.86 $\mu$m physical pixel size. On the other hand, the exit plane is imaged onto the pickoff camera by some optical elements. The pickoff camera calibration is based on the idea that in vacuum the width measured on the pickoff camera and on Vcam5 should be the same. Thus we fit a Gaussian (azimuthally symmetric) onto the two camera pictures and define the "calibration factor" as width$_{Vcam5}$/width$_{pickoff}$. Because there are ten measurements in each set, we again take the average of the calibration factor and this quantity too will have an uncertainty as displayed below in the table and the plot. Moreover, it turns out that the calibration factor is not the same for all the vacuum measurements - it has an energy dependence that is outside the statistical uncertainty. Therefore the picture I have envisioned about the measurement is clearly too simplistic again, there are factors affecting the picture of the pickoff camera other than simple geometrical optics. Nevertheless I will progress by creating a calibration curve once more using the energies of the vacuum meaurements, the calibration factors and interpolation. I will again

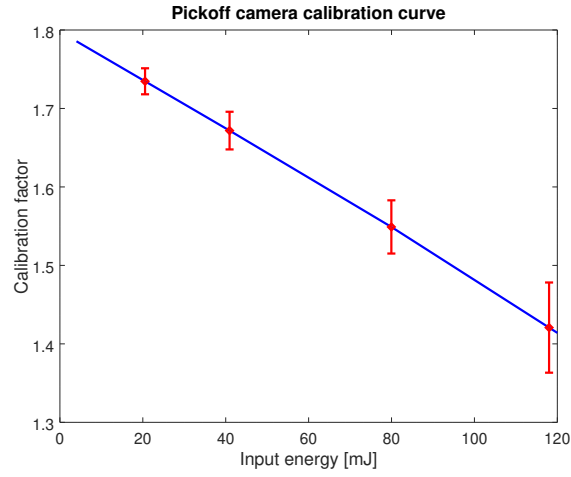extrapolate for low energy values.



Figure 7: Calibration curve for distribution width for pickoff camera. Red diamonds with error bars mark the calibration points obtained from the vacuum measurements.

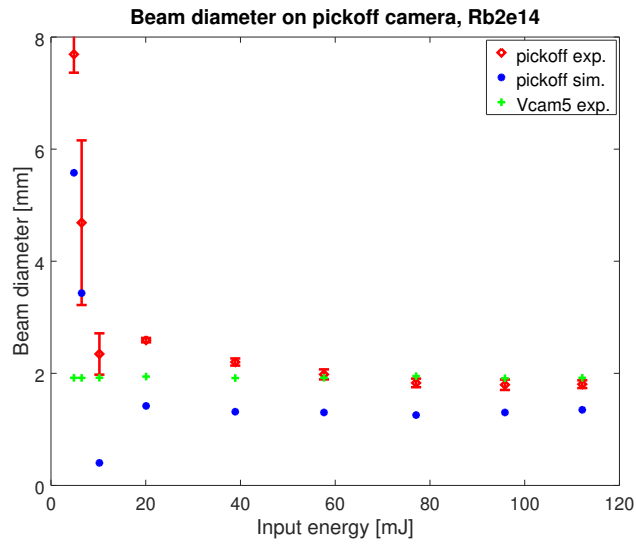And finally here is the plot the measured and calulated beam diameters, the measured values have errorbars:



Figure 8: Measured and calculated beam diameters. The numbers are the beam diameter of the azimuthally symmetric Gaussian beam that best fits the distribution. The width of the beam on the virtual exit is also shown.

## Different plasma densities

I have repeated the calculations for two other plasma densities, using the same method for obtaining the initial parameters of the input gaussian beam. I will skip making a table here, I just present the output energy and output pulse diameteter plots:

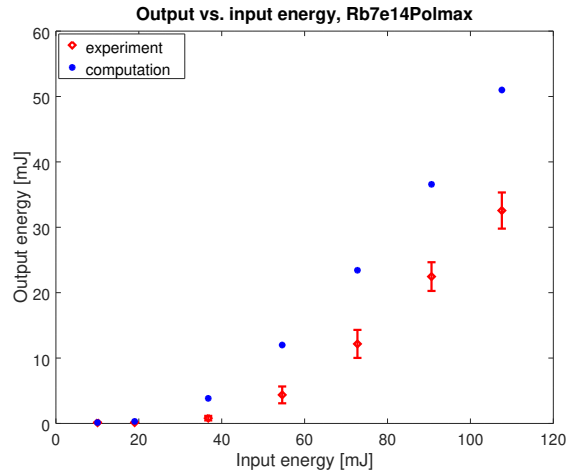For the $\mathcal{N} = 7 \times 10^{14}/\mathrm{cm}^3$ measurement:



Figure 9: Outgoing pulse energy vs. input pulse energy for the $\mathcal{N} = 7 \times 10^{14}/\mathrm{cm}^3$ calculation
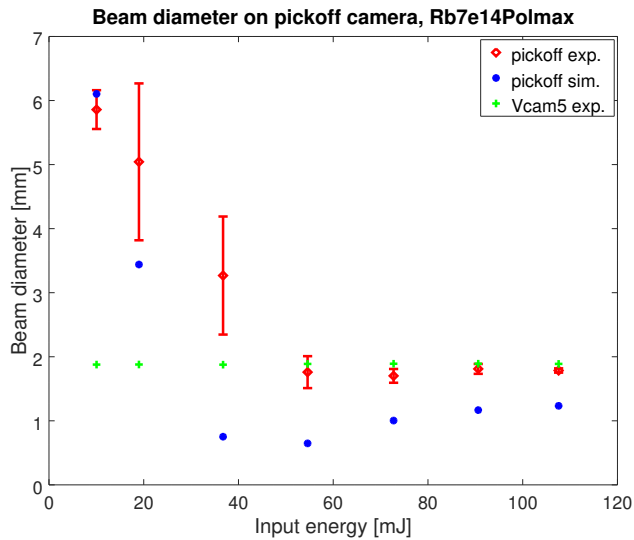


Figure 10: Measured and calculated beam diameters. The numbers are the beam diameter of the azimuthally symmetric Gaussian beam that best fits the distribution. The width of the beam on the virtual exit is also shown.

And the $\mathcal{N} = 1 \times 10^{15}/\text{cm}^3$ measurement:
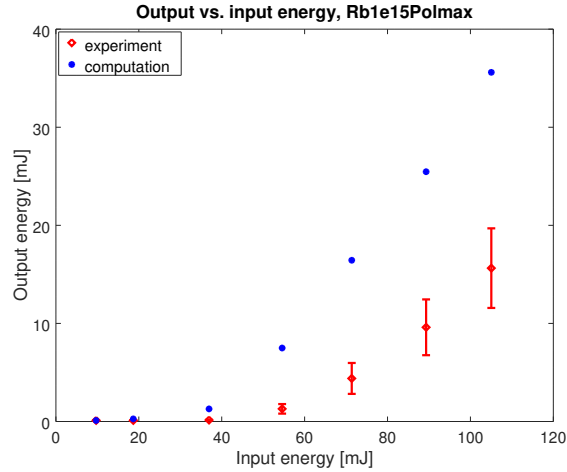


Figure 11: Outgoing pulse energy vs. input pulse energy for the $\mathcal{N} = 7 \times 10^{14}/\text{cm}^3$ calculation
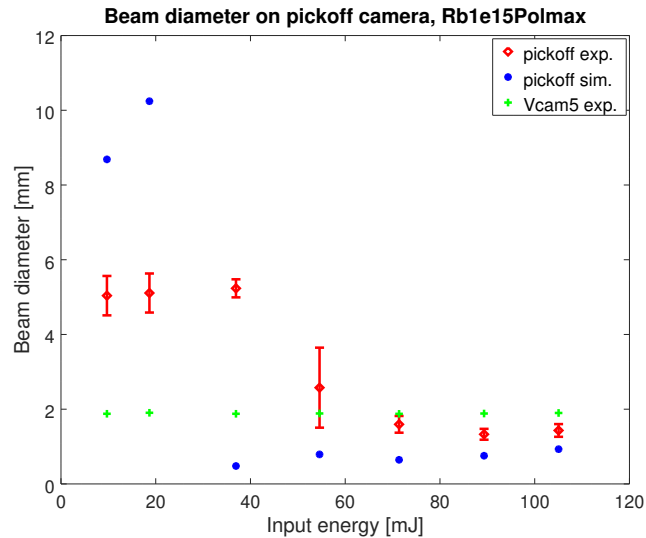


Figure 12: Measured and calculated beam diameters. The numbers are the beam diameter of the azimuthally symmetric Gaussian beam that best fits the distribution. The width of the beam on the virtual exit is also shown.

## Discussion

The figures show that the simulation does reproduce qualitatively the tendencies followed by the input energy and pulse width, but is quantitatively not very good. The output energy is overestimated and the beam width is underestimated by a considerable factor. A qualitative explanation can of course be

9

offered: the real experimental beam is not a Gaussian. Even if it could be considered azimuthally symmetric, a non-gaussian beam (e.g. a flattened gaussian) will diverge more, diffract in a wider radius than the nicest zero order gaussian. That means that the beam will be wider and more energy will be lost when creating a wider plasma channel than that calculated by the simulation with a zero order gaussian input.

The "breakthrough" can nevertheless be well identified when the output energy starts increasing from some very small values. This is the place where the beam width is the narrowest. The approximate location is the same for the calculation and the measurement, but a more "dense" set of measurements with respect to energy could give us a better picture.

There are a number of issues that prevent a precise comparison at the moment even if the calculation is repeated with a more realistic input (which I intend to do anyway).

- The energy calibration of the output energy meter is somewhat ad-hoc, the fact that it depends on the input energy and is not merely some geometric factor suggests that there is something systematic we would have to take into account.

- Using a Gaussian fit and taking its width is also not a simple question. We have some very "non-gaussian" distributions, a nonlinear fit will sometimes converge to different parameters depending on the initial parameter set. Maybe some parameter that is not a fit like a "half-energy radius" or a "90% energy radius" would be better (the radius around the maximum which contains half or 90% of the pulse energy).

- I have in fact tried calibrating the width of the distribution on the pickoff to that on the virtual exit a different way as well. I have integrated in one direction and used a 1D Gaussian to fit the resulting linear distribution. I got very different calibration factors for the x and y directions. When I derived calibration factors from the x-direction of the virtual exit to the y-direction of the pickoff and vice versa (as if the image on the pickoff was rotated by 90 degrees) I got two factors which were much closer, but still quite different. Their average was very close to the calibration factors produced with the 2D fit, but it does suggest that apart from rotational transformations there must also be an amount of "skewness" somewhere.

- The difference between the measurement and the calculation is best where the vapor is less dense - which suggests that maybe I should repeat calculations with denser vapor (stonger nonlinearity) with more stringent accuracy requirements.
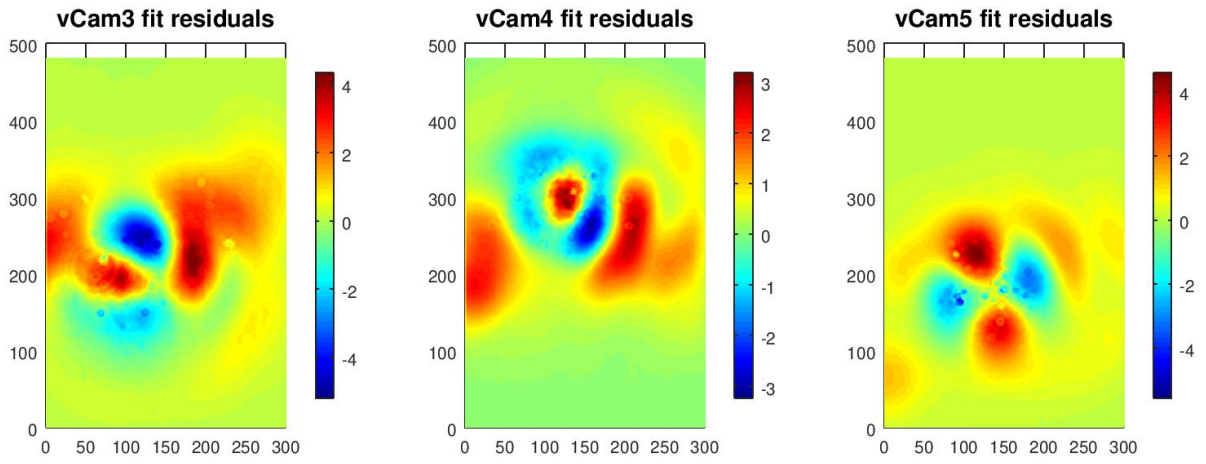
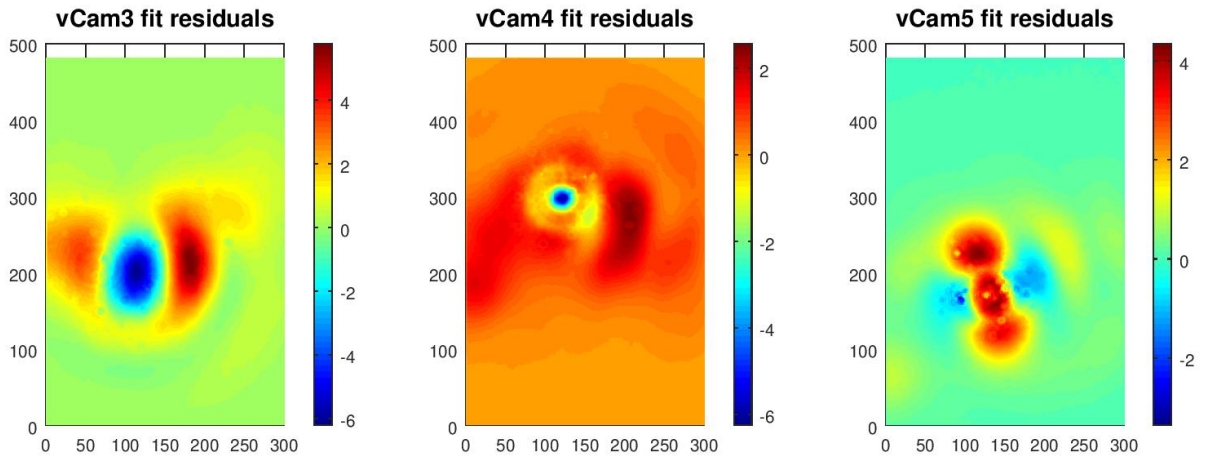Figure 13: Gaussian beam fit normalized residuals.



Figure 14: Flattened Gaussian beam fit, N=6 normalized residuals.